



**QUEEN'S
UNIVERSITY
BELFAST**

A new method of constructing drug-polymer temperature-composition phase diagram relevant to the hot-melt extrusion platform

Tian, Y., Jones, D., Donnelly, C., Brannigan, T., Li, S., & Andrews, G. (2017). A new method of constructing drug-polymer temperature-composition phase diagram relevant to the hot-melt extrusion platform. *Molecular Pharmaceutics*, 1-39. <https://doi.org/10.1021/acs.molpharmaceut.7b00445>

Published in:
Molecular Pharmaceutics

Document Version:
Peer reviewed version

Queen's University Belfast - Research Portal:
[Link to publication record in Queen's University Belfast Research Portal](#)

Publisher rights

Copyright © 2017 American Chemical Society. This work is made available online in accordance with the publisher's policies. Please refer to any applicable terms of use of the publisher.

General rights

Copyright for the publications made accessible via the Queen's University Belfast Research Portal is retained by the author(s) and / or other copyright owners and it is a condition of accessing these publications that users recognise and abide by the legal requirements associated with these rights.

Take down policy

The Research Portal is Queen's institutional repository that provides access to Queen's research output. Every effort has been made to ensure that content in the Research Portal does not infringe any person's rights, or applicable UK laws. If you discover content in the Research Portal that you believe breaches copyright or violates any law, please contact openaccess@qub.ac.uk.

Determining Risk of Barrett's Esophagus and Esophageal Adenocarcinoma Based on Epidemiologic Factors and Genetic Variants
A new method of constructing drug-polymer temperature-composition phase diagram relevant to the hot-melt extrusion platform

Yiwei Tian, David S. Jones, Conor Donnelly, Timothy Brannigan, Shu Li, Gavin P. Andrews*

*** Corresponding author address:**

Professor Gavin Andrews
Pharmaceutical Engineering Group,
School of Pharmacy,
Queen's University Belfast,
97 Lisburn Road,
Belfast, BT9 7BL,
United Kingdom.
Email: g.andrews@qub.ac.uk

ABSTRACT

Current experimental methodologies used to determine the thermodynamic solubility of an API within a polymer typically involves establishing the dissolution/melting endpoint of the crystalline API within a physical mixture, or through the use of the glass transition temperature measurement of a de-mixed amorphous solid dispersion. The measurable “equilibrium” points for solubility are normally well above the glass transition temperature of the system meaning extrapolation is required in order to predict the drug solubility at pharmaceutical relevant temperatures. In this manuscript we argue that, the presence of highly viscous polymers in these systems results in experimental data that exhibits an under or over estimated value relative to the true thermodynamic solubility. In previous work we demonstrated the effects of experimental conditions and their impact on measured and predicted thermodynamic solubility points. In the light of current understanding, we have developed a new method to limit error associated with viscosity effects for the application in small-scale hot-melt extrusion (HME). In this study HME was used to generate an intermediate (multi-phase) system containing crystalline drug, amorphous drug/polymer rich regions as well as drug that was molecularly dispersed in polymer. An extended annealing method was used together with high-speed differential scanning calorimetry to accurately determine the upper and lower boundary of the thermodynamic solubility of a model drug –polymer system (felodipine and Soluplus®). Comparing to our previously published data, the current results confirmed our hypothesis that the prediction of the liquid-solid curve using dynamic determination of dissolution/melting endpoint of the crystalline API physical mixture presents an under estimation relative to the thermodynamic solubility point. With this proposed method, we were able to experimentally measure the upper and lower boundary of liquid-solid curve for the model system. The relationship between inverse temperature and drug-polymer solubility parameter (χ) remained linear at lower drug loadings. Significant higher solubility and miscibility between felodipine-Soluplus® system were derived from the new χ values.

INTRODUCTION

Amorphous solid dispersions (ASDs) are one of several enabling formulation strategies employed to overcome the poor aqueous solubility of BCS class II/IV drugs. The feasibility of the amorphous form to enhance solubility and dissolution performance is routinely assessed from pre-formulation stages to late clinical trial¹. Interestingly, despite significant research having been conducted in the area of ASDs the selection of excipients including polymers for this purpose is still largely based on a trial and error approach. An added complexity in formulating ASDs is in selection of an appropriate manufacturing method. ASDs have been commonly manufactured using spray-drying or hot melt extrusion (HME). Recently HME has received considerable attention due to it being continuous in nature, it is solvent-free and permits ease of scale. However, HME is relatively complex in that an operator may change a number of process variables (e.g., feed rate, screw speed, barrel temperature, screw design), which may impact upon the final quality of the ASD. Therefore, the successful manufacture of an ASD using HME requires a rational approach to formulation design, processing and parameter selection.

The application of the Flory-Huggins (F-H) theory to produce thermodynamic phase diagrams has gone some way to provide improved understanding of the solubility of drug in both small molecular matrix (1, 2) and large polymeric dispersion systems (3-6). This method has the potential to be used to identify design space for the manufacture of stable ASD systems, particularly for non-ambient processes such as HME and may help to reduce the cost of drug product manufacture (7). Currently, the experimental methodologies used to understand drug solubility in polymeric carriers comprises two principal approaches; the 'thermodynamic' equilibrium point determined from dissolution/melting of a crystalline drug in a polymer/drug physical mixture or the 'thermodynamic' equilibrium point determined from a de-mixed supersaturated amorphous polymer/drug solid dispersion (8-10). To explain this further, a thermodynamic phase diagram shown in Figure 1 depicts a black solid line as the true thermodynamic drug solubility equilibrium curve in respect to the polymer. This indicates the lowest energy for the mixture. In both methods a dynamic heating approach is normally used, and the

dissolution/melting of the crystalline drug within the physical mixture or the glass transition temperature of the de-mixed amorphous solid dispersion may be identified using differential scanning calorimetry (DSC). The de-mixing method, involves a supersaturated amorphous solid dispersion (amorphous polymer with a drug loading $\geq 80\%$ w/w) which is annealed at a range of temperatures that are lower than the melting point of the drug and higher than the glass transition temperature of the system (10). Therefore, the supersaturated amorphous system undergoes de-mixing to lower energy (via direction a to e in Figure 1). After de-mixing (reported to be approximately 4 hours for an indomethacin-PVP system (11)) the temperature of the single glass transition is used to calculate drug solubility from a constructed drug-polymer T_g -composition curve. In contrast, the dissolution/melting endpoint measurement method measures the end point of the dissolution/melting temperature of crystalline drug within physical mixtures of polymer at a constant heating rate (via direction of c to e in Figure 1). In both approaches, although careful sample preparation and judicious choice of experimental conditions can improve the accuracy of both methods, the presence of highly viscous polymeric materials significantly impacts upon the determination of thermodynamic equilibrium solubility values. For example, in using the de-mixing method, a phase separated two T_g system may be observed after a prolonged period of annealing (12, 13). The appearance of amorphous-amorphous systems is the initial indication of a non-equilibrium state of the de-mixing process due to the presence of high viscosity polymers, thus extended de-mixing times may be required for the full crystallisation of an amorphous-amorphous system. Achievement of equilibrium in such systems may be require a long period of time, particularly at the latter stages of the de-mixing process due to this isothermal experimental design and a progressively increasing viscosity. The measured data may therefore overestimate the true thermodynamic equilibrium solubility (dash line, Figure 1). Furthermore, different preparation techniques (milling, film casting or spray drying) may also introduce differences in the initial state of the amorphous system, in which the rate of de-mixing will vary (14, 15). In this study, attempts were made to utilize the de-mixing method for determination of the equilibrium solubility in a FD-Soluplus system. However, for an 80% w/w FD-Soluplus

ASD prepared by DSC quench-cooling, annealing at 120°C required at least 8 hours to generate a distinctive glass transition with the presence of a small drug melting peak. Moreover, the use of T_g values for the determination of drug composition is extremely difficult as amorphous FD and Soluplus exhibit glass transition values within 30°C of each other and the signal to noise ratio at high drug loading is very low (data shown in supporting documentation). For other systems a de-mixing method may be entirely inappropriate, i.e. felodipine, celecoxib or indomethacin with low T_g polymers (Eudragit EPO®) where the T_g of the polymer is indistinguishable to the T_g of the amorphous drug (16). In comparison, the accuracy of the measurement when using the dissolution/melting endpoint method may be improved by suitable sample preparation and the use of slow heating rates (17). Common methods of preparing drug and polymer mixtures before DSC analysis include ball milling and cryomilling. The main advantage of milling and mixing is that the effects of diffusive mixing are reduced and a more accurate value of the dissolution/melting endpoint may be obtained. A greater extent of homogeneity is often obtained when samples are prepared via milling as opposed to physical mixing using a mortar and pestle. The reduction in the effects of diffusive mixing improves crystalline drug dissolution kinetics, and the prediction of the thermodynamic solubility curve may be more accurate. The completion of dissolution will always be delayed however by the presence of a viscous polymeric material; thus the measured temperature for the endpoint may be greater than the true thermodynamic equilibrium curve (dash dot line). This results in an underestimation of drug solubility in polymer as shown in Figure 1.

Despite the variation in the data generated by the alternative approaches described above, both can provide useful information regarding the evaluation of the drug-polymer interaction parameter, and the relevance of temperature and drug composition upon the miscibility within binary amorphous solid dispersions. Thermodynamic phase diagrams together with an appreciation of the dynamics of amorphous drug crystallisation can be used to further improve our understanding of the manufacturing process and phase stability of binary amorphous drug-polymer solid dispersion systems (18, 19). The

construction of thermodynamic drug-polymer temperature-composition phase diagrams relies heavily on the empirical relationship that exists between the drug-polymer interaction parameter, χ , and the temperature, T . As a result of slow heating rates ($< 5^\circ\text{C}/\text{min}$) employed in the dynamic dissolution/melting endpoint approach, it is common that melting point depression data can be obtained only at drug loadings greater than 70% w/w if the system exhibits favourable miscibility (20, 21). In order to complete the liquid-solid transition curve, the relationship between χ and $1/T$ is utilised to determine the entropic (A) and enthalpic (B) contributions to χ , so the interaction parameter can be calculated for any temperature below the limit of detection in the DSC (eq.1).

$$\chi_{drug-poly} = A + \frac{B}{T} \quad (1)$$

The extrapolation of the solubility curve is dependent on the assumption of A and B calculated on the basis of a linear relationship between χ and $1/T$. To date, all drug-polymer phase diagrams completed in the literature have exhibited Upper Critical Solution Temperature (UCST) behaviour (5, 8, 22) where $A < 0$ and $B > 0$. This situation arises when the value of the interaction parameter decreases as temperature is increased. An example of a plot of χ vs. $1/T$ associated to UCST behaviour can be observed in Figure 2. From such a plot, it would be extremely desirable to obtain drug solubility data at lower temperatures. The attainment of additional data points beyond previously accepted limits of detection would undoubtedly further our understanding of crystalline drug solubility and amorphous drug miscibility within the polymer. Consequently, the extension of our understanding of χ vs. $1/T$ will enable further evaluation of whether UCST behaviour adequately describes the drug-polymer system at the lower temperature range (23).

In this article we utilise HME in an attempt to address the aspects described above and to generate a highly mixed drug polymer solid dispersion containing multi-phases. Using this approach, in combination with high heating rates to determine crystalline content, will provide useful insights for the determination of the liquid-solid boundary beyond the current limit of

understanding and those developed thus far using the two aforementioned methods. Furthermore, the multi-phase system and annealing results may help provide a clearer understanding of drug-polymer miscibility and importantly, the impact that processing conditions may have upon the drug polymer platform.

MATERIALS AND METHODS

Crystalline felodipine (FD) form I was purchased from Taresh Chemicals Ltd. (Co. Down, UK) and used without further purification. Polyvinyl caprolactam-polyvinyl acetate-polyethylene glycol graft copolymer (brand name Soluplus®) was obtained from BASF Chemical Co. (Ludwigshafen, Germany). Samples were kept in a temperature controlled vacuum oven (50°C) for at least two days prior to experiments.

Ball Milling

Ball milling was performed at room temperature using a Retsch MM200 oscillatory ball mill (Mohrengasse, Germany). A physical mixture (1g) containing 60% w/w felodipine was prepared and placed into a 25 mL milling chamber with a single stainless steel ball ($\Phi=15\text{mm}$) and milled at 20Hz. A milling cycle of two minutes was followed by a stationary period of two minutes. In total, 8 minutes of ball milling were completed. This period of ball milling has previously been found to maximise the particle surface interaction between felodipine and Soluplus® and render the drug partially amorphous (5).

Hot-Melt Extrusion

A fractional 2-level scope design incorporating drug load (50-70% w/w FD), screw speed (11-30rpm), 90° mixing elements (0-3) and 60° mixing elements (0-3) was examined. Screening of these parameters was used to determine the significance of each factor on drug-polymer mixing and crystalline content (Design Expert 9, Stat-Ease Inc., MN, USA). These experimental variables were identified as the key parameters that would influence drug-polymer interaction when processed via a co-rotating 10mm twin-screw hot-melt

extruder (Microlab10mm, Rondol, France). The 2-level scope design produced the experimental design detailed in Table 1. Drug and polymer mixtures (5 g) were initially hand mixed with a pestle and mortar. These physical mixtures containing 50% and 70% w/w FD were then fed into the extruder, which was maintained at a temperature of 130°C.

After carefully selecting the screw configuration and speed, extrudates were manufactured containing 60-90% w/w felodipine with Soluplus® at a temperature of 130°C ($T_g \leq T_{\text{process}} \leq T_{\text{end}}$) and a screw speed of 11rpm. The intension of using the HME to prepare the mixture is to produce a multiple phase system consisting of amorphous drug, amorphous polymer, crystalline drug and amorphous drug-polymer solid dispersion, therefore, the feeding rate was kept at slow speed (5 mg/min) to maximize the natural convey from twin screw extrusion process. The prepared mixture can also be benefited from zero moisture content, which may be considered as important factor in determination of drug-polymer equilibrium point in thermal analysis.

The extruder was not fitted with a die to limit the backpressure and to maximise yield. Extrusion at these conditions ensured that residual crystalline felodipine remained in the formulation. Each extrudate sample was then characterised using high performance differential scanning calorimetry (HyperDSC) and Raman chemical imaging.

Thermal Analysis

Differential scanning calorimetry (DSC 8000 Perkin-Elmer, United Kingdom) was used throughout this study for dissolution/melting endpoint determination. For dissolution/melting endpoint experiments, 1°C/min was used. Extrudates containing 70-90% w/w felodipine manufactured using a full conveying set-up were scanned to evaluate the effects of sample preparation by HME as opposed to ball milling through analysis of the heat of fusion (ΔH_{fus}) of the respective FD melting endotherms. At this low heating rate, nitrogen was selected as the purge gas and the temperature and cell constant calibration were carried out using high purity indium, lead and zinc.

Following extrusion (full conveying), samples were annealed at elevated temperatures for a period of 24 hours. During isothermal annealing, the heat flow as a function of time was evaluated. Using this approach, endothermic or exothermic transitions were expected due to dissolution of crystalline drug into the mixture or recrystallisation of amorphous drug from the mixture, respectively.

High heating ramp rates utilizing power compensation were used following annealing. In brief, samples were rapidly equilibrated to -60°C and ramped to 200°C at a rate of 200 °C/min in an attempt to detect any remaining crystalline FD. As a comparison, freshly extruded samples were also examined using the same heating rate. Helium was used as a purge gas at a flow rate of 40 ml/min. Calibration of the instrument at this heating rate was completed using indium, lead and zinc reference samples. In all DSC analyses, samples weighing as close to 5.5 mg were placed into aluminium sample pans with a crimped pinhole lid. To ensure annealing (124-139°C) did not result in degradation of the sample, heat and hold experiments were performed using thermogravimetric analysis (TGA, TA Instruments, United Kingdom) over a time period of 24 hours and the weight loss of each formulation was determined to be less than 1% (attributed to the water loss).

Powder X-Ray Diffraction (PXRD)

The polymorphic form of drug within extrudates was evaluated using a MiniFlex II powder X-Ray diffractometer (Rigaku, United States). The radiation was generated from a copper source operating at 40kV and 40mA. The FD-Soluplus® samples were cryomilled and packed onto a zero background sample holder and scanned from 0° to 40° 2 θ , using a step width of 0.01° 2 θ and a scanning rate of 1°/min in continuous mode.

Raman Chemical Mapping

Extruded FD-Soluplus® samples were pressed onto aluminum discs and Raman Mapping was performed using a Raman Microscope 300 (Perkin Elmer, United Kingdom). All analyses were completed using an exposure time of 6 seconds (3 x 2s) in the wavenumber range from 200-3200 cm⁻¹. Mapping

areas of approximately 400 μm^2 were obtained using a x20 objective with a laser diameter of 50 μm and spacing of 25 μm . Spectral data analysis was performed using Grams/AI version 7.02 from Thermo GalacticTM (Waltham, MA). Maps produced using this methodology were compared to the spectrum of pure crystalline FD and correlation factors were calculated using Raman Image software.

Rheological Characterisation

The dynamic viscosities of FD-Sol mixtures at 1Hz were determined using an AR2000 Rheometer (TA Instruments, United Kingdom). Physical mixtures weighing 250 mg were loaded on to a lower stationary plate held at 145 °C. An upper geometry consisting of a 20mm parallel plate was employed with the gap between the upper and lower plates set at 400 μm . The samples were allowed to equilibrate at 145 °C for a period of 5 minutes. When this time had elapsed, the samples were cooled at a rate of 5°C/min to the target temperature of 125 °C. An oscillatory stress, selected from the linear viscoelastic region, of 5 Pa, was employed for these non-destructive tests. This test was selected to represent the conditions similar to the DSC annealing study.

Construction of Phase Diagram

An in-depth discussion of the theory behind the construction of thermodynamic drug-polymer phase diagrams is provided in our previous published articles and hence only a brief explanation is given here (5, 8). The midpoint values of the upper and lower boundaries identified from annealing were used in equation 1 to determine the respective χ values at each temperature.

$$\frac{1}{T_m} - \frac{1}{T_{m0}} = -\frac{R}{\Delta H} \left(\ln \phi_{drug} + \left(1 - \frac{1}{m}\right) \phi_{poly} + \chi_{drug-poly} \phi_{poly}^2 \right) \quad (2)$$

A plot of χ versus 1/T enabled calculation of the associated entropic (A) and enthalpic (B) contributions to χ (eq1). The determination of these values facilitated the extrapolation of the remainder of the liquid-solid transition curve

at points beyond the limit of experimental detection. The position of the spinodal curve was constructed by calculating the second derivative of equation 4 and equating to zero (24)

$$\Delta G_{mix} = \Delta H_{mix} - T\Delta S_{mix} \quad (3)$$

$$\Delta G_{mix} = RT \left(\phi_{drug} \ln \phi_{drug} + \frac{\phi_{poly}}{m} \ln \phi_{poly} + \chi_{drug-poly} \phi_{drug} \phi_{poly} \right) \quad (4)$$

Substitution of the previously calculated values of A and B into the second derivative of equation 2 enabled a series of theoretical spinodal curve temperatures to be calculated for a range of drug volume fractions.

RESULTS AND DISCUSSION

As the pre-mixing technique used in this study was HME, Soluplus® was an ideal excipient due to its low T_g (80°C) and suitable melt flow at a temperature of 130°C. At this extrusion temperature, the polymer will be in its rubbery state, however the drug will not have exceeded its melting point. Theoretically, as the materials are conveyed through the barrel of the extruder, the crystalline drug will be mixed throughout the rubbery polymeric matrix. However, the shear stresses produced by the mixing action of the co-rotating screws could potentially cause felodipine to be rendered partially amorphous and encourage dissolution in the polymer matrix (25). It is also possible that during extrusion drug could solubilise depending on the solubility of the drug-polymer system. The purpose of employing a 2-level fractional factorial design was to rapidly understand the effect of screw configuration on the residual crystalline content of FD-Sol extrudates. The application of the factorial design (2^{4-1}) resulted in 8 extrusion trials. Each extrudate from this DoE was analysed using a combination of HyperDSC and Raman Spectroscopy. In each trial we were interested in determining whether there was crystalline felodipine present post-extrusion (Table 1).

Characterisation of Melt Extrudates

The incorporation of mixing elements (60 or 90°) to the screw configuration at a temperature of 130°C led to the production of an amorphous solid dispersion for 50% FD-Sol. When a full conveying screw configuration was used crystalline FD was detected in all extrudates, demonstrating the effectiveness of 90° and 60° kneading elements in generating amorphous content and/or drug dissolution in the polymer. This observation holds significance to the production of ASDs via non-ambient processing (26). By incorporating mixing elements, lower extrusion temperatures can be selected, yet amorphous solid dispersions may still be produced as a result of the shear imparted by the mixing elements.

Based upon observations made during our initial DoE, a full conveying screw configuration was used to manufacture 50-90% w/w FD-Sol mixtures. This

was essential in attempting to detect the position of the liquid-solid transition curve at low drug loadings i.e. 50% w/w FD. It would have been possible to use mixing elements at higher drug loads, since crystalline FD would still be present, post-processing. However, in the interests of continuity in the pre-mixing stage, no kneading elements were utilised when extruding these mixtures. Upon exiting the extruder, fresh samples of FD-Sol ranging from 50-75% w/w drug were characterised using both Raman chemical mapping and HyperDSC. Extrudate samples were mapped and correlated to the spectrum of pure crystalline FD with a high correlation being represented by red or white in the rainbow lookup table. The presence of crystalline FD (Form I) was evident in Raman maps of samples (Figure 3). The presence of amorphous FD was also evident in Raman maps shown in support information. The heat of fusion from melting of residual crystalline FD was also evident in each sample using HyperDSC conducted at 200°C/min (Figure 4). The areas showing high correlation to reference crystalline FD spectrum indicate the presence of crystalline FD (red - white), whilst the areas showing low correlation to reference crystalline (opposite colour map in Figure 3) are general representing the amorphous FD (supporting information). The intension of producing a multi-phase system consisting of amorphous drug, crystalline drug, and amorphous drug-polymer solid dispersion has been achieved.

An isothermal annealing experiment at elevated temperatures followed by a DSC temperature ramp (typically conducted at a heating rate of 10 °C/min), to analyse residual crystal content, has previously been utilized to determine the equilibrium solubility of drug in polymer (17). It is noted however, that under low heating rates within the DSC, there are at least two events occurring simultaneously, dissolution of drug into the polymer carrier and melting of crystalline drug. The dissolution of crystalline drug into polymer may occur when the temperature exceeds the T_g of the polymer (amorphous drug-polymer mixture), which is lower than its crystalline melting temperature. It is possible that a relatively low heating rate such as 10 °C/min could therefore facilitate the dissolution of crystalline drug into polymer and a melting endotherm may not be detectable. In contrast, using high speed DSC and

Raman mapping, detection of crystalline content in extrudates containing low drug loads (55% and 50% w/w) is possible, e.g. for 50% w/w FD-Soluplus extrudate, a heat of fusion peak ($\Delta H_{\text{fus}} \approx 0.19$ J/g) was observed and crystalline FD domains, approximately 50 μm , were observed. Additionally, PXRD was utilized and peaks (Figure 5) characteristic of crystalline felodipine (Form I) were observed in the samples containing 60-90% w/w drug however it was difficult to verify the presence of crystalline felodipine in the extrudates containing at drug loadings of 55% and 50% w/w.

The magnitude of the heat of fusion is significantly influenced by the sample preparation technique (Figure 6). For example, a ball milled sample with a drug loading of 90% w/w FD produces a ΔH_{fus} value of 30.79 J/g at heating rate of 1°C/min. However, significantly lower energy (9.25 J/g) is required to cause fusion of felodipine within an extruded sample containing the same drug loading. Similar effects are observed in the samples containing other drug loadings. These findings indicate that hot-melt extrusion provides greater mixing of drug and polymer to a state where the drugs are readily solubilised within the polymer matrix prior or during the DSC experiment. The process of HME therefore induced a greater degree of miscibility between drug and polymer when compared to ball milling. Moreover, the effects of diffusive mixing are minimised within the samples prepared via HME as opposed to ball milling. For the purposes of this study, a 24-hour annealing time was applied to all extruded samples and the heat flow baseline was monitored so that the position of equilibrium solubility could be plotted with greater confidence.

Experimental determination of liquid-solid transition curve

Figure 7 illustrates thermograms for 65% and 60% FD-Sol melt extrudates using the extended annealing approach and high heating rates (200 °C/min). The initial high speed DSC scans for both melt extrudates confirmed the presence of a multi-phase system consisting of amorphous drug, polymer, mixed drug and polymer and crystalline drug (Figure 7a (number 1 and 5)). To experimentally detect the boundary for liquid-solid transition curve of FD-Sol at different drug loadings, an extended annealing experiment was carried out at various temperatures. When a suitable temperature was applied at defined

drug loading, the system will rest in equilibrium state indicating by a stable heat flow curve (as function of time) in the DSC thermogram. For example, as shown in the Figure 7a, after extended annealing at different temperatures, specifically 125°C (Figure 7a-2), 127°C (Figure 7a-3) and 130°C (Figure 7a-4) for 65% w/w drug loading and 123°C (Figure 7a-6) and 125°C (Figure 7a-7) for 60% w/w felodipine loading, respectively. It is clear that a single-phase system was generally observed with distinctive glass transitions and absence of melting endotherm peak when higher annealing temperature was applied (Figure 7a-4,7). For the 65% w/w drug loaded system, a melting endothermic peak was observed at annealing temperatures of 125°C and 127°C, whilst a small endothermic peak was observed at 123°C for the 60% drug loaded system. Increasing the temperature to 130°C for 65% and 125°C for 60% drug loaded samples, respectively, there were no melting endotherms observed indicating complete dissolution of drug into the polymer (much lower than the melting temperature of pure felodipine). The aim of annealing the sample at different temperatures was to define the lowest temperature required to fully solubilise drug in polymer. Therefore, at this temperature and drug loading, the amorphous solid solution is at its equilibrium state, i.e. the lowest Gibbs free energy state ($\Delta G < 0$) of the binary system. It is noted that the melting of crystalline FD lattice is an endothermic event however, the annealing temperatures utilised in this study are well below melting point of the drug ($T < T_m$). Thus a dissolution event rather than a melting of drug predominates during annealing. An exothermic heat flow therefore may be expected during the isothermal annealing as the crystalline FD continuously dissolves within the polymer until a saturated homogenous solid solution is obtained ($\Delta H - T\Delta S < 0$). With this in mind, a followed high speed scan can be used to identify the presence of undissolved crystalline FD. As demonstrated in Figure 7b, for both 65% and 60% drug loaded systems, an exothermic heat flow curve (endothermic up, zero heatflow is marked in dash line) was observed at all selected temperatures corresponding to the Figure 7a, however only samples annealed at the higher temperatures (130°C for 65% w/w and 125 for 60% w/w) will exhibit a single glass transition with the absence of melting event (Figure 7a-4,7). It would also be expected that crystalline FD within the extrudate would promote the process of

recrystallisation/drug-polymer de-mixing if the annealing temperature was below the liquid-solid line (27, 28). Using these findings for the 65% drug loaded sample it is clear that the experimental liquid-solid transition line exists within the region of 127-130°C, i.e. the boundary of the liquid-solid transition curve may be obtained. TGA analysis verified that these isothermal time periods within the solubilisation regime did not result in the thermal degradation of drug.

The selected annealing temperatures for extrudates containing 60%-90% w/w felodipine can be found in Table 2. With this data, the position of the liquid-solid transition curve for FD-Sol was experimentally constructed at lower drug loadings than previously published data. Using the original phase diagram constructed by ball milling followed by thermal analysis (1°C/min) and application of the FH theory (5), a comparison can be made between the positions of the liquid-solid transition curves produced by each method (Figure 8). Indeed, our hypothesis has been confirmed that the liquid-solid line produced using the dynamic approach resulted in an underestimation of the equilibrium solubility of felodipine within Soluplus when compared to the data obtained using the current method. For example, the methodology laid out in this study found that the liquid-solid transition curve existed between 137 and 139°C at a composition of 90% w/w drug loading, whereas the dynamic approach previously described by our group has identified the equilibrium solubility at approximately 141°C at the same drug loading. Similarly at 70% w/w felodipine loading, a melting point of approximately 135°C was identified previously, whereas this study located the liquid-solid line between 130 and 133°C.

The underestimation in equilibrium drug solubility predicted by the F-H theory has previously been discussed (8, 29). Insufficient drug-polymer mixing, produced by the process of ball milling has been found to strongly influence values of T_{end} when DSC heating rate is varied. Careful consideration of the selection of DSC heating rate when utilising the melting point depression approach is therefore essential. Increased DSC heating rates will result in the broadening of endothermic melting events and will produce lower values of

crystalline drug solubility and amorphous drug miscibility than would have perhaps been expected. Application of common DSC heating rates 0.2-10°C/min will also result in varying times above the T_g of the parent polymer. By extending this time within the solubilisation regime, it is possible that drug dissolution into the polymeric carrier will be enhanced at lower DSC heating rates. However, it is also suggested that the intensive drug-polymer mixing that takes place within the extruder barrel will reduce the inhibitory effects of diffusive mixing when the samples are annealed in the DSC. Furthermore, an isothermal period of 24 hours is expected to provide a sufficient time frame to allow the dissolution of the crystalline drug into the polymeric matrix when compared to traditional DSC timescales. This may seem excessive, however this study aimed to identify the extent of the crystalline solubility underestimation and performing this annealing stage was essential in this process. Lastly, this methodology is not affected by the thermal lag between sample and reference pans as a result of increasing heating rate. The modified technique, using HyperDSC to detect for the presence of crystalline felodipine, has provided an improvement in identification of boundary for the drug solubility curve of felodipine-Soluplus blends.

Rheological evaluation

The effects of polymer viscosity also have to be considered when experimentally determining the position of the liquid-solid transition curve using thermal analysis techniques. Increasing polymer content results in an increase in viscosity of the drug-polymer mixture. Sun *et al.* (2010) found that their improved analytical method (annealing between 4 and 10 hours followed by a 10°C/min DSC scan) produced a liquid-solid transition curve approximately 7°C lower than that determined by a DSC scanning approach, extrapolated to zero heating rate, for mixtures containing 30% and 40% drug (17). The discrepancies identified at these relatively low drug loadings were attributed to the effects of polymer viscosity. With increased viscosity, it is imperative that drug-polymer mixtures are given sufficient time to reach equilibrium solubility. Otherwise, reduced molecular mobility will hinder the dissolution of the drug within the polymer and equilibrium may not be achieved within the limited time frame provided by a standard DSC heat ramp.

The dynamic viscosities of felodipine-Soluplus amorphous solid dispersions within the solubilisation regime of this system are shown in Figure 9. With decreasing drug load, it can be observed that significant increases in dynamic viscosity are produced across the temperature range of 125-145°C. For example, the dynamic viscosity of 90% w/w drug loaded sample at the processing temperature of 130°C is approximately 340 Pa.s. However, the dynamic viscosity of 50% w/w FD-Sol at the same temperature was found to be in excess of 4000 Pa.s. It is noted that the rheological methodology employed in this work involves producing ASDs at elevated temperatures before calculating dynamic viscosity. By melting the drug within the rubbery polymer, it is likely that the drug will plasticise the polymeric carrier. This does not mirror the HME process that has been applied in this study; instead this information provides an indication of the viscosity values of the plasticised polymer and drug mixtures at various drug loadings. Nevertheless, such a significant increase in dynamic viscosity with polymer content illustrates how an underestimation in the position of the liquid-solid transition curve may be obtained within the timescales of dynamic DSC single scan techniques. With such large dynamic viscosity values being measured when polymer content is increased, extended annealing times at elevated temperatures above polymer T_g will encourage the dissolution of the drug into the polymeric matrix and the likelihood of the attainment of equilibrium solubility will be enhanced. In this study, all of the upper boundaries of the liquid-solid transition curve exhibited a single T_g upon heating at 200°C/min after annealing and did not possess melting endotherms relating to crystalline felodipine. These findings suggest that the annealing periods of 24 hours at the temperatures specified in Table 1 are not only sufficient to overcome the effects of polymer viscosity but have also produced a single equilibrium drug-polymer phase.

Construction of thermodynamic drug-polymer phase diagram

The identification of the upper and lower boundaries of the liquid-solid curve has been completed for felodipine loadings between 60-90% w/w whereas melting point depression data had only been detected for felodipine-Soluplus systems as low as 70% w/w in a previous study. By inputting the midpoint values of the upper and lower boundaries of the liquid solid curve into

equation 1, a range of χ values were collected. In order to calculate the entropic (A) and enthalpic (B) contributions to, a plot of χ versus $1/T$ was constructed, as shown in Figure 10.

It can be observed from Figure 10, a comparison of the values of χ at the same drug load that the methodology developed in this study not only produced more negative χ values for drug-polymer system but also exhibited a lower slope (B values) in equation 1 when compared to the dynamic method. Furthermore, the whole position of the curve has moved to lower temperatures relative to our previously published results, obtained using a dynamic method. This may be used to further support our postulation that, in the dissolution/melting point approach, the viscosity of the polymer will delay the completion of drug melting process, hence a higher temperature is normally observed. Although negative χ values do signify the existence of numerous adhesive bonds between the drug and polymer, larger, more negative values of the interaction parameter give an indication of a more favourable thermodynamic driving force towards the miscibility of the drug and polymer at temperatures close to the melting point of the drug.

Such discrepancies in the χ values of the same drug-polymer system have previously been discussed. Sun et al. 2010 reported a χ value for Nifedipine-PVPK12 system as -2.5 (17) whereas Marsac et al. 2009 (4) calculated the single χ value for this drug-polymer mixture as 0. The differences in the calculations were attributed to the methodology used to determine the values of crystalline solubility in the polymer. A negative χ value was calculated when cryomilling was used to pre-mix the drug and polymer, followed by annealing at elevated temperatures for timescales ranging between 4 and 10 hours. However, the dynamic approach of scanning physical mixtures at $1.0^{\circ}\text{C}/\text{min}$ to elucidate melting point depression data resulted in a value of $\chi=0$ being calculated for the Nifedipine-PVPK12 system. It was rationalised that cryomilling produced a greater degree of uniformity and a reduction in particle size of the drug-polymer system. Furthermore, annealing of these samples at times exceeding traditional DSC timescales facilitated drug dissolution at lower temperatures than identified via a dynamic approach. These effects

describe the situation in this study where the incorporation of HME, extended annealing periods and HyperDSC resulted in more negative χ values than the dissolution/melting point approach. By ramping physical mixtures using DSC heat scans, as a result of the unfavourable dissolution kinetics and insufficient timeframe to allow complete dissolution of the drug, it is possible to realise that the melting event may mask the true thermodynamic solubility point (annealing temperatures at defined drug loadings).

Analysis of Figure 10 shows that the value of χ becomes more negative for each plot as temperature is increased, which is again indicative of UCST behaviour (24). This finding holds particular significance since the region between 60-70% w/w felodipine-Soluplus was previously unidentified. Despite the improved sensitivity of the method detailed in this study, the liquid-solid transition curve could not be identified at drug loadings beneath 60% w/w. Figure 10 illustrates the discrepancies in the entropic (A) and enthalpic (B) contributions to χ as a result of methodology to determine the position of the liquid-solid transition curve. These values are essential for the completion of the equilibrium solubility curve to low drug loadings where experimental determination was not possible. Linearity was assumed in the dynamic method at drug loadings lower than 90% w/w felodipine content with a correlation coefficient (r^2) of 0.99 being obtained. The new method of HME, annealing and HyperDSC exhibited linear behaviour at drug loadings less than 80% w/w FD producing an r^2 value of 0.90.

The dissolution/melting approach produced values of -14.419 and 5744.7 for A and B, respectively, whereas the combination of HME, annealing and HyperDSC determined these values of A and B as -11.163 and 4150.7, respectively. The liquid-solid transition curve for the new methodology was extrapolated to low drug loadings and its position can be compared to that of the previous approach in Figure 11a. It can be observed that lower experimental temperatures of the liquid-solid transition curve impacts significantly on the extrapolation to lower drug loadings. These findings can be attributed to the discrepancies in the entropic and enthalpic contributions to χ resulting from the plot in Figure 10. Furthermore, the position of the spinodal

curve was calculated using the second derivative of equation 4. A comparison of the positions of the spinodal curves for the new and dynamic methodologies can be found in Figure 11b.

It can be observed that significant discrepancies in the respective positions of the spinodal curves exist at pharmaceutically relevant temperatures. For example, at a temperature of 25°C, the dynamic method predicted that a weight fraction of approximately 12% w/w FD would remain stable in the amorphous mixture, whereas the new methodology described here suggests a value of approximately 22% w/w. The spinodal curve provides an indication of the limit of thermodynamic metastability and its position provides a potential method for rational selection of drug weight fraction for a ASD formulation. As a result of more accurate determination of the position of the liquid-solid transition curve, and therefore the entropic and enthalpic contributions to χ , it is evident that a larger weight fraction of FD may be less susceptible to phase separation and crystallisation at pharmaceutically relevant temperatures than what was previously determined using the dissolution/melting point approach.

The concept of introducing the theoretic spinodal curve is for the potential application of phase separation in the drug-polymer solid dispersion systems. It is imperative to aware that the apparent miscibility between amorphous drug and amorphous polymer (two liquids) is often much higher than the thermodynamic solubility (equilibrium) of the binary system. If we consider the crystallization of the drug from amorphous solid dispersion being two-step process, the liquid-liquid phase separation to form drug rich amorphous droplets would be the pre-cursor for the crystallization of the drug from ASD. Therefore, the relevance of drug loading and temperature of the ASD at different positions of the phase diagram may be significantly altered resulting different mechanisms of liquid-liquid phase separation, i.e. the rate of phase separation will be different (spinodal vs. binodal).

In this drug-polymer combination case, the liquid-solid line is above the whole theoretical spinodal curve. Therefore, from the pure thermodynamic point of view, when a system sits underneath the solubility curve, it is not equilibrium. The prepared ASD below the solid-liquid line (pharmaceutical relevant conditions) will undergo crystallization and/or phase separation as matter of

time (Figure 11a). However, when the polymer is involved in the ASD, the viscosity and potential low mobility of the system below the glass transition will also prolong the process of ASD returning to its equilibrium state, the mechanisms of which may be highly relevant to the position of binodal and spinodal curve.

Significance of Pre-mixing via HME

In order to demonstrate the importance of incorporating HME in the determination of crystalline equilibrium solubility, a physical mixture of 60% Felodipine-Soluplus was annealed at a temperature of 125°C for a period of 24 hours. Using fast scanning (define rate) after a period of isothermal annealing (define conditions) it is evident that residual FD crystal remained present within the system (data not shown). However, this temperature signified the upper boundary of the liquid-solid transition curve when an extruded sample of 60% FD-Sol containing crystalline was annealed at 125°C. This finding demonstrates the importance of incorporating HME over ball milling in this methodology in order to overcome the effects of diffusive mixing/unfavourable kinetic conditions. Theoretically, if this ball-milled sample were annealed for an infinite period of time at 126°C, the residual FD crystal would eventually dissolve into the polymeric matrix as a result of the favourable thermodynamic conditions. However for the purpose of screening a polymer for ASD, using HME permits, improved accuracy within a shorter experimental timeframe.

General discussion

In this study, a new approach has been presented for drug-polymer solubility determination in relation to HME platform, in which felodipine and Soluplus were mixed within a hot-melt extruder and annealed at elevated temperatures over a 24-hour period. Subsequent high speed DSC scanning enabled the liquid-solid line to be defined more accurately than previous methods. In the original DSC dynamic approach, drug-polymer mixtures are commonly prepared via ball milling or cryomilling. This process will induce particle surface interaction and a degree of amorphous content. However in this case, preparation of extrudates using a co-rotating extruder with full

conveying screw configuration resulted in significantly lower ΔH_{fus} values required to melt the remaining crystalline drug content than those required after the process of ball milling (Figure 6). After annealing these samples for 24 hours, it is extremely likely that if drug crystals remain, the annealing temperature does not signify the point of the liquid-solid transition curve, as this approach should provide ample time for drug dissolution to overcome the effects of polymer viscosity within the multiphase system.

Selection of an extrusion temperature of 130°C resulted in the presence of felodipine crystals in the extrudate. This is an essential requirement of this approach since HyperDSC has been used to detect the boundaries of the liquid-solid transition curve based on the presence of felodipine crystals at a scan rate of 200°C/min. This heating rate provides enhanced sensitivity when compared to standard DSC heating rates, for example 1.0-10°C/min, and it will reduce the potential dissolution of the crystalline drug into the polymer providing a more accurate representation for the point of equilibrium solubility (30). When constructing thermodynamic drug-polymer phase diagrams using the F-H theory, it is common that melting point depression data can only be detected for drug loadings $\geq 70\%$ w/w. It may be possible to elucidate melting temperatures for lower drug loadings for systems that exhibit a limited degree of miscibility. It has previously been observed that felodipine–Soluplus possessed relatively favourable miscibility when compared to Felodipine-HPMCAS. Melting point depression data could only be detected as low as 70% w/w FD-Sol when a dynamic DSC method was utilised in comparison to 55% w/w used in FD-HPMCAS [7]. Hence to further construct the phase diagram, a linear relationship between interaction parameter and temperature was assumed. However, by applying annealing and HyperDSC at scanning rates of 200°C/min, it was possible to experimentally determine the position of the liquid-solid transition curve at 60%FD w/w. It was observed that the relationship between χ and temperature remained linear in this previously undefined region. Ideally, experimental data for the liquid-solid transition curve could be detected across the entire range of possible drug loadings when applying this modified method with increased sensitivity. Before consideration of alternative polymeric carriers, it should be stressed that polymorphic

transformations of the crystalline drug are possible when processing in a hot-melt extruder and adequate characterisation of the extrudates is essential post-processing to ensure that the correct polymorphic form of the drug exists within the excipient. One important point of note with regards to the methodology presented in this study is the amount of drug that is required. The process of HME in the Rondol Microlab requires approximately 5 grams of material for each composition. Preformulation studies will not always be performed with excess amounts of material (31) . If small amounts of drug are available and the purpose of collecting experimental data is purely to compare the extent of interaction between drug and polymeric excipients, the dynamic approach would suffice as long as the same conditions are applied across different drug-polymer combinations. However, for this study, key aims were to fully understand the difference between a dynamic approach and the thermodynamic equilibrium point of drug-polymer solid solution system, the relationship between thermodynamic miscibility and kinetic impact of process conditions. Therefore it was essential to carry out HME as a pre-mixing step in order to understand the mechanism of this small-scale platform. Furthermore, it is recognised that the time taken for sample preparation with HME (residence time < 2 minutes) in this study is much quicker than typical ball mill and cryomill preparation and the yield after HME is high due to the self-wiping co-rotating screw design. Given the high level of mixing induced via the extrusion process and the extensive annealing step, this method will result in much more accurate calculations of drug solubility. This new approach will also enable polymer screening to take place, provided that drug-polymer mixtures are given sufficient time above polymer T_g to reach equilibrium solubility. The detrimental effects of increasing viscosity as a result of high polymer content causing underestimations in melting point depression are also overcome using this methodology. Therefore, it is likely that equilibrium solubility of the drug in a polymeric excipient will be obtained in a shorter timeframe than 24 hours after being subjected to HME. This study has demonstrated, for the first time, the use of HME followed by extensive annealing and HyperDSC to overcome the limitations of a dynamic approach to probe the thermodynamic solubility of a small crystalline molecule within a high viscous polymeric carrier. This highly sensitive methodology will provide

a much more accurate depiction of the equilibrium solubility curve position as shown in Figure 8 and 11. It also demonstrated that the effects of kneading configuration and relevance to the drug composition and temperature for further mechanistic understanding of HME as a means of developing robust continuous manufacturing platforms for the production of stable amorphous solid dispersion systems.

CONCLUSION

The development of an improved methodology in determining the position of the liquid-solid transition curve of a drug-polymer system and its relation to the use of hot-melt extrusion technology have been explored in this study. The limitations associated with detecting melting point depression data have been discussed at length where the effects of diffusive mixing and heating rate selection hinder the accuracy of traditional methods. In order to enhance the uniformity of felodipine-Soluplus® mixtures prior to processing using dynamic thermal analysis methods, we have demonstrated that HME can be incorporated to generate a multi-phase mixture with uniform dispersion. Design of Experiment (DoE) was employed to carry out a 2-level scope design so that drug-polymer uniform mixtures could be manufactured yet residual crystalline felodipine retained in the extrudate. Characterisation of the fresh extrudates containing 50-90% w/w felodipine were completed using a combination of Raman Spectroscopy, HyperDSC and PXRD. After validating the presence of crystalline FD (form I) in each of the samples, mixtures were annealed at various temperatures for a period of 24 hours to assess the thermodynamic solubility point. This process demonstrated the extent of the underestimation of FD solubility in Soluplus when utilising the dynamic DSC method. Subsequently, as a result of the increased sensitivity and accuracy, it was possible to define the relationship between χ and $1/T$ at lower drug loadings than previously reported. It was observed that a linear relationship between χ and $1/T$ exists at drug loadings ranging from 60-75% w/w felodipine-Soluplus system. Calculation of the entropic and enthalpic contributions to χ enabled extrapolation of the remainder of the liquid-solid transition curve below 60% w/w drug loading. Discrepancies between the positions of the FH predicted liquid-solid transition curves using each methodology were presented with a clear underestimation for dynamic heating approach being identified.

Table 1. A 2-level factorial design (Design Expert 9) for HME processing. The presence of crystalline FD within extrudates was identified using both HyperDSC and Raman spectroscopy. Materials were extruded at 130°C

Run No.	No. 90° Mixing Elements	No. 60° Mixing Elements	Screw Speed (rpm)	Drug load (% w/w)	Crystalline content
1	0	3	30	50	No
2	3	3	30	70	Yes
3	0	0	11	50	Yes
4	3	3	11	50	No
5	3	0	30	50	No
6	0	3	11	70	Yes
7	3	0	11	70	Yes
8	0	0	30	70	Yes

Table 2. Selected annealing temperatures for extrudates containing 60-90% w/w FD. The upper boundary identifies the temperature where no crystalline FD was detected using HyperSC following 24 hours of annealing whilst the lower boundary signifies the temperature where a melting endotherm was present.

Drug Load (% w/w)	Annealing Temperature (°C)	
	Upper boundary (°C)	Lower boundary (°C)
90	139	137
85	137	136
80	136	134
75	135	133
70	133	130
65	130	127
60	126	123

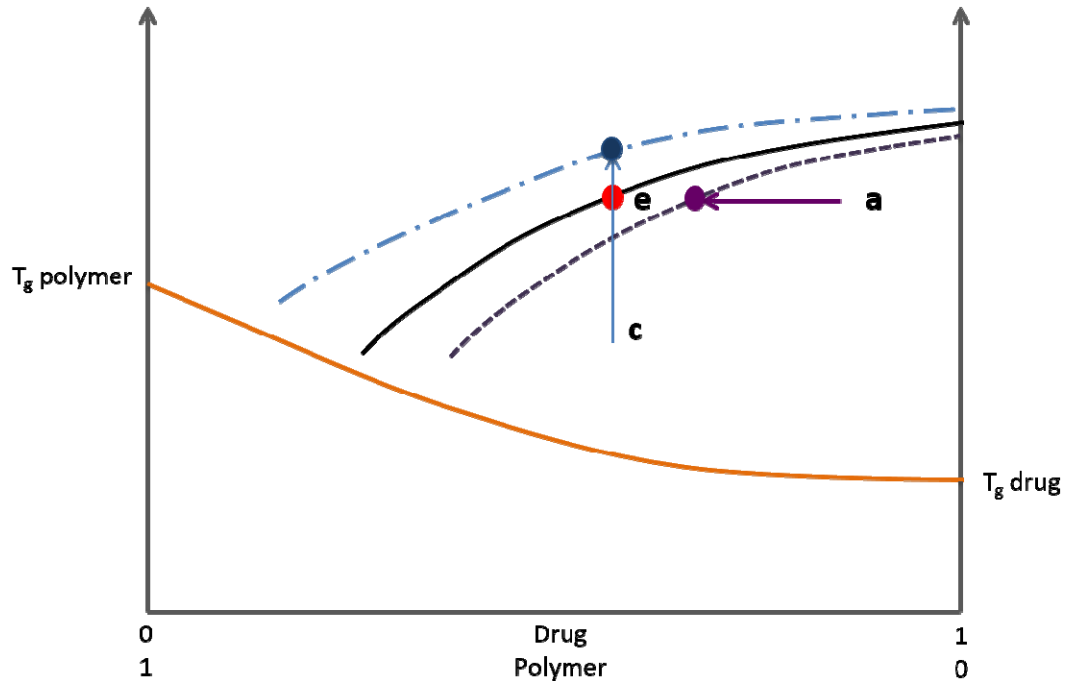


Figure 1. The illustration of thermodynamic drug-polymer solubility curve (solid line), measured “equilibrium” drug-polymer solubility curve via demixing method (short dash line) and measured “equilibrium” drug-polymer solubility curve via drug dissolution end point.

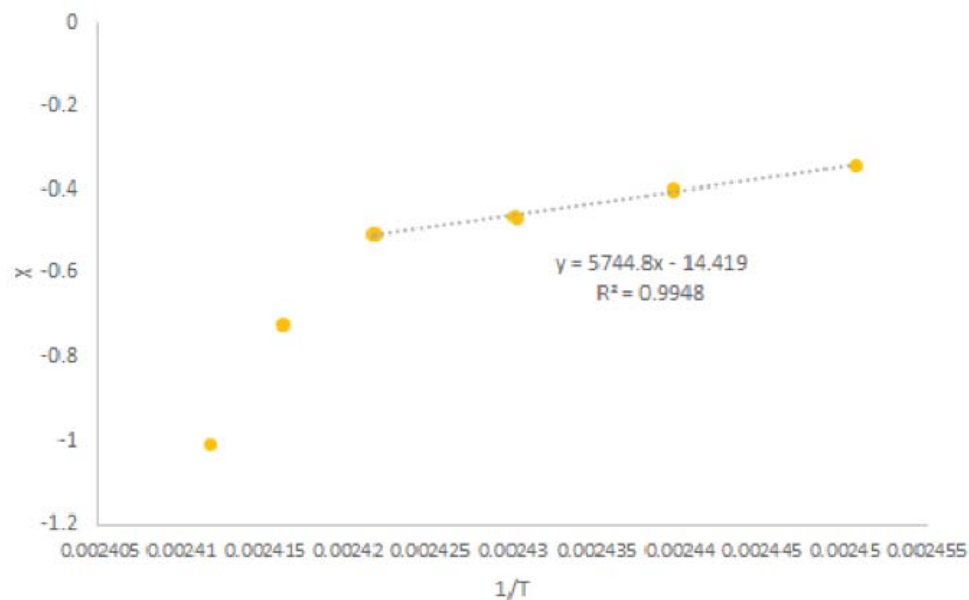


Figure 2: A plot of χ versus $1/T$ constructed using melting point depression data for 70-95% w/w FD-Sol mixtures processed at $1.0^{\circ}\text{C}/\text{min}$. Data taken from Tian et al. 2012 [7].

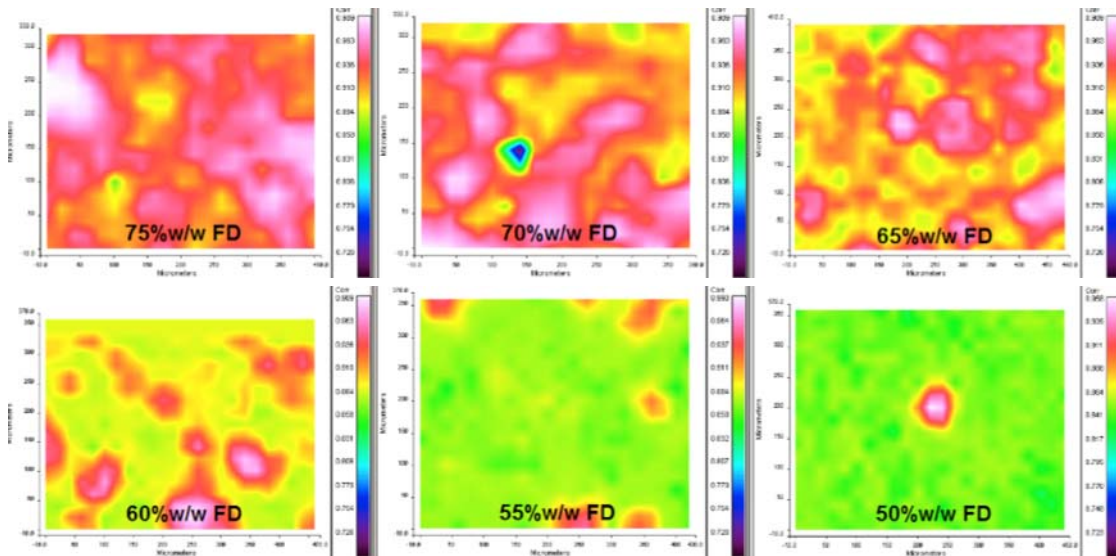


Figure 3: Raman mapping images of FD-Soluplus® extrudates. 100% FD type I crystal was used as a reference spectra and varying degrees of FD crystals can be observed. Brightly shaded areas (white/pink) identify the presence of FD polymorph form I crystal.

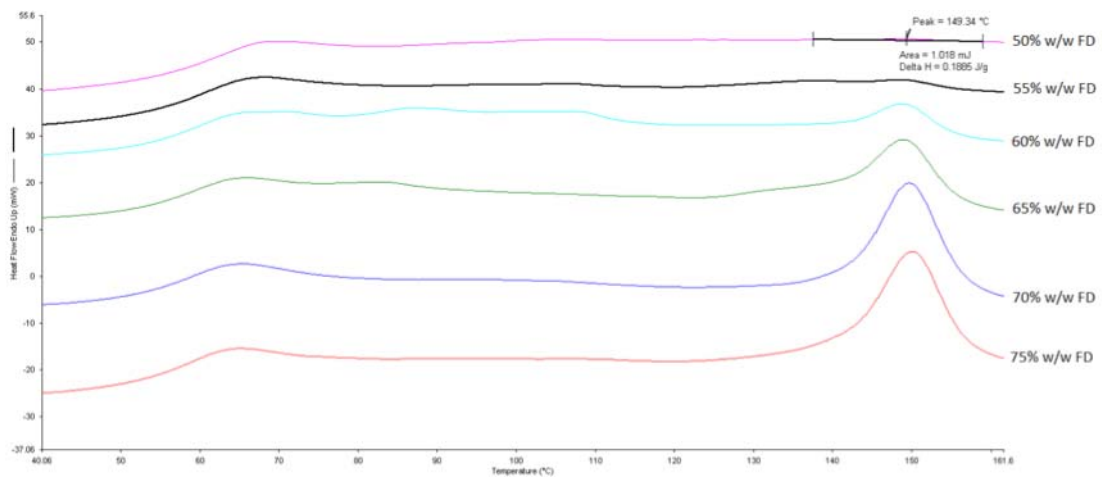


Figure 4: HDSC thermograms of freshly prepared extrudate containing 50-75% w/w FD completed using a heating rate of 200°C/min.

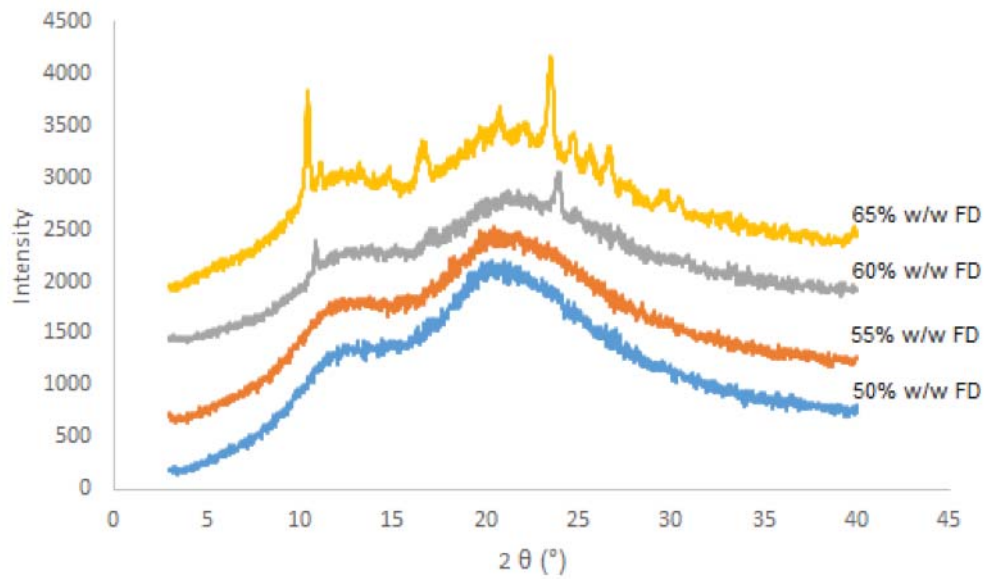


Figure 5: PXR D diffractograms of freshly prepared 50-65% w/w FD-Sol extrudates.

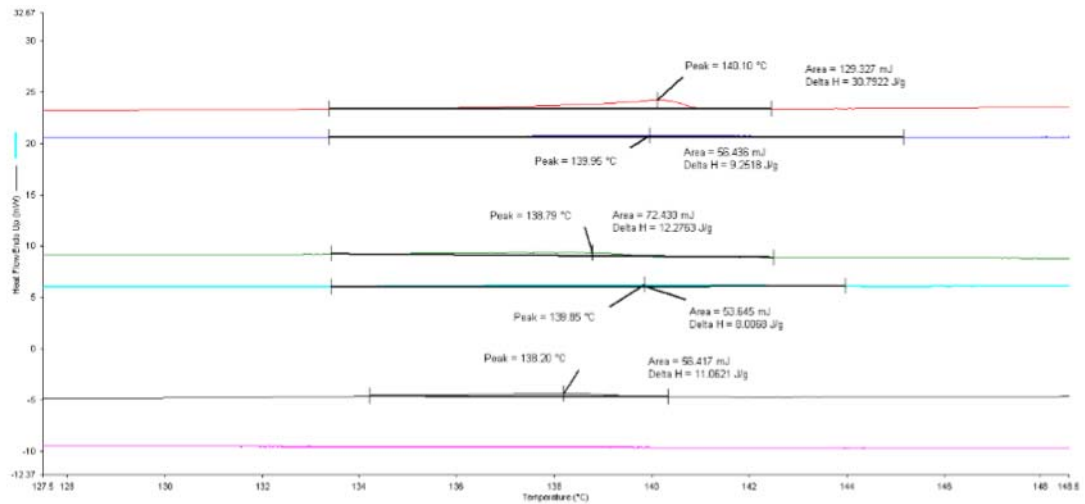


Figure 6: DSC thermograms of ball milled physical mixtures and hot melt extruded formulations at a scanning rate of 1C/min (From top to bottom: 90% BM, 90% HME, 85% BM, 85% HME, 80% BM and 80% HME w/w FD).

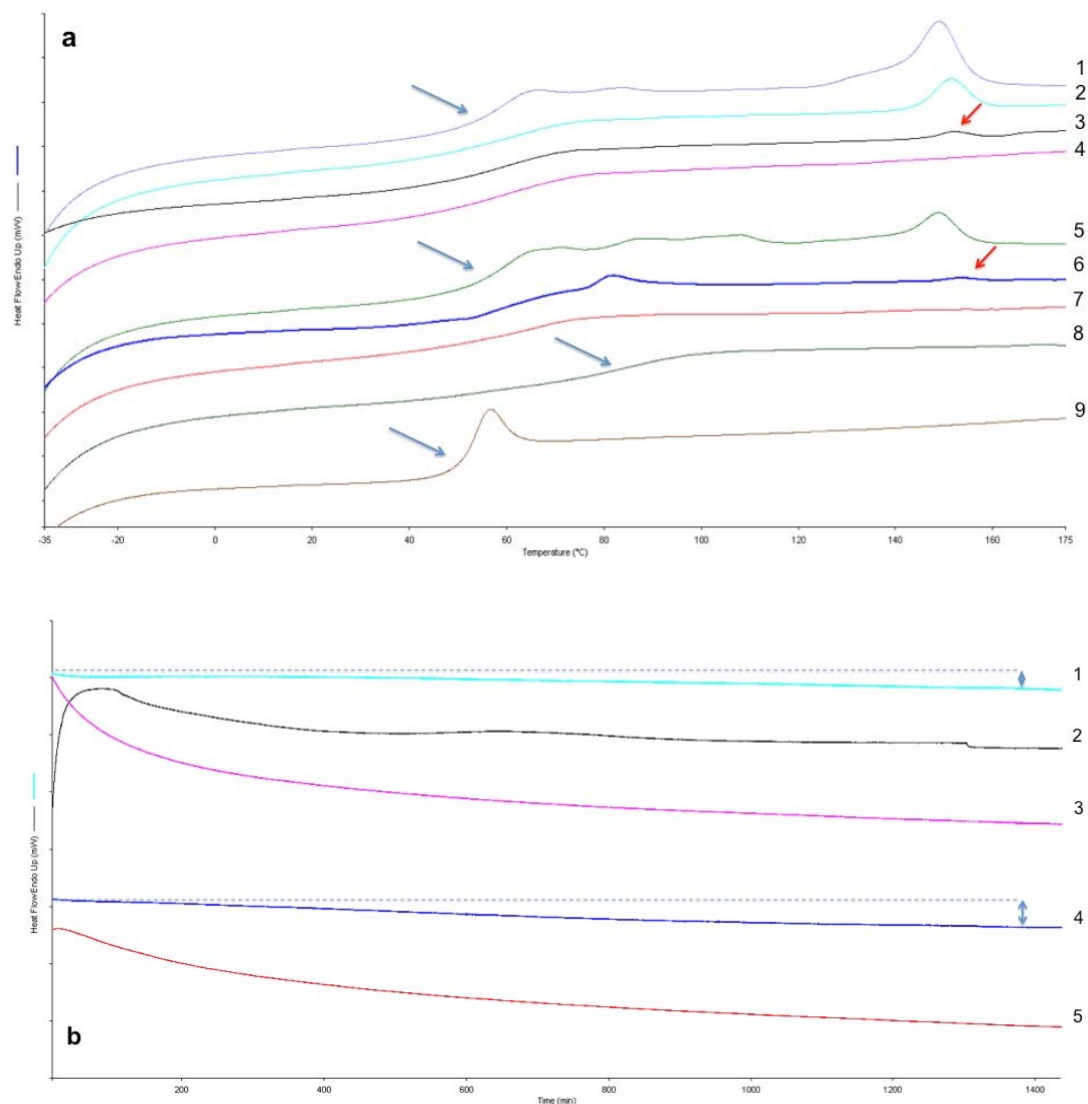


Figure 7: (a) HyperDSC thermograms of 65% (1-4) and 60% (5-7) w/w FD-Sol extruded samples before and after a period of 24 hours of annealing at elevated temperatures: fresh prepared HME of 65% (1) and 60% (5) FD-Solu, annealed at 125 °C (2), 127 °C (3) and 130 °C (4) for 65%FD-Solu; annealed at 123 °C (6) and 125 °C (7) for 60%FD-Solu; (8) pure polymer Soluplus (9) pure amorphous FD (b) The heatflow signal of 65%FD-Solu annealed at 125 °C (1), 127 °C (2) and 130 °C (3); 60%FD-Solu annealed at 123 °C (4) and 125 °C (5).

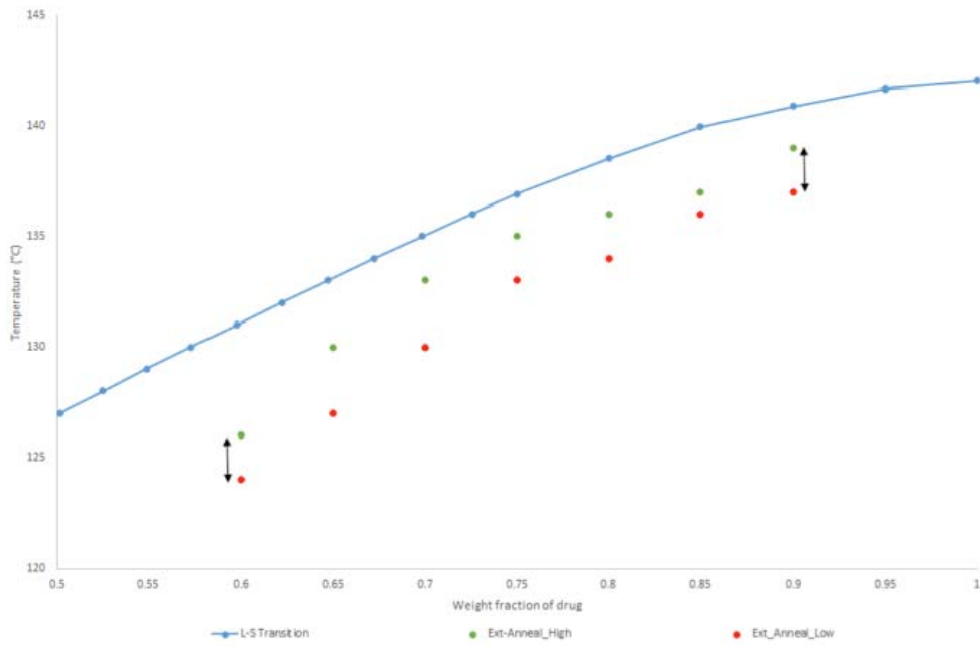


Figure 8: A comparison between the positions of the liquid-solid transition curve calculated using melting point depression data from the dynamic method and the upper and lower boundaries of equilibrium solubility identified via HME, annealing and HDSC.

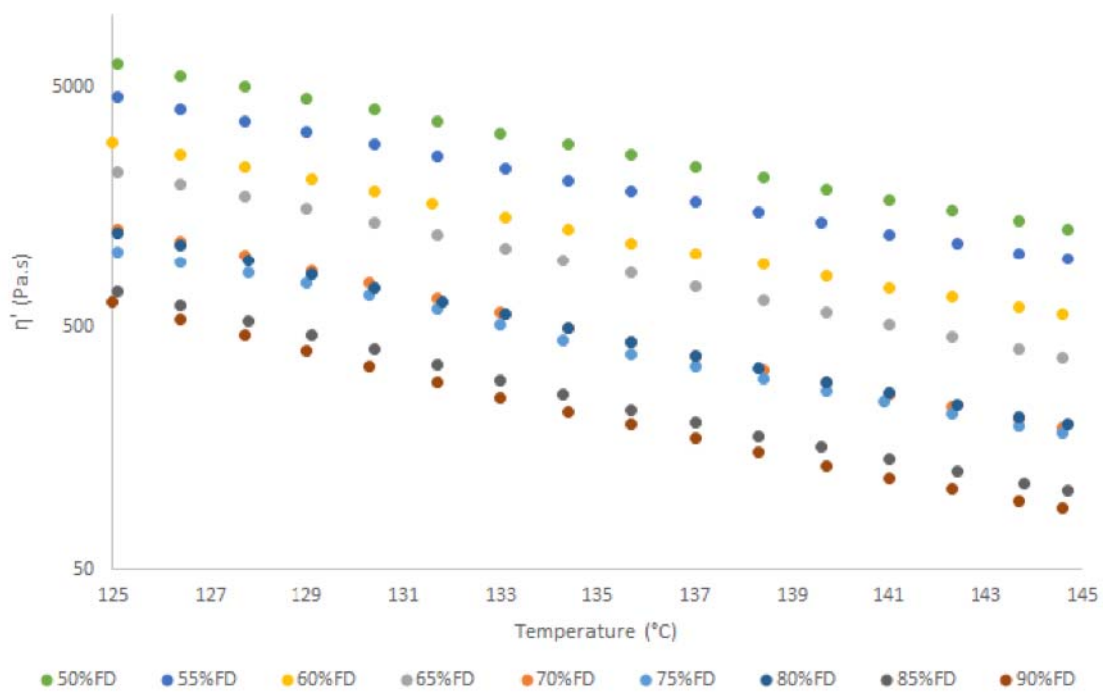


Figure 9: Dynamic viscosities of 50-90% w/w FD-Sol physical mixtures after melting at 145°C and cooling to 125°C at a rate of 5°C/min, oscillation stress of 5Pa and frequency of 1Hz.

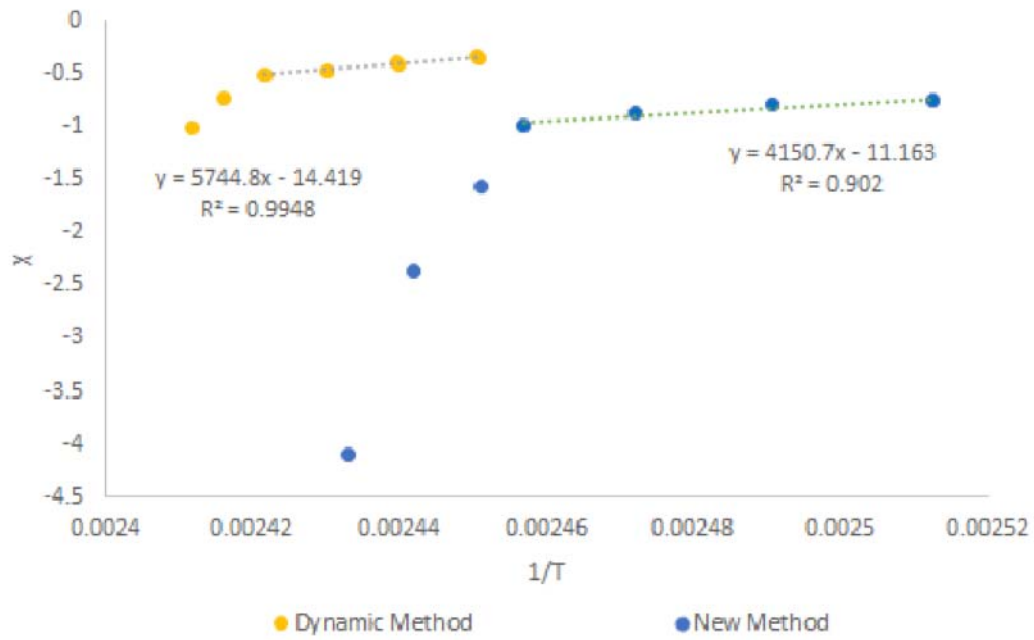
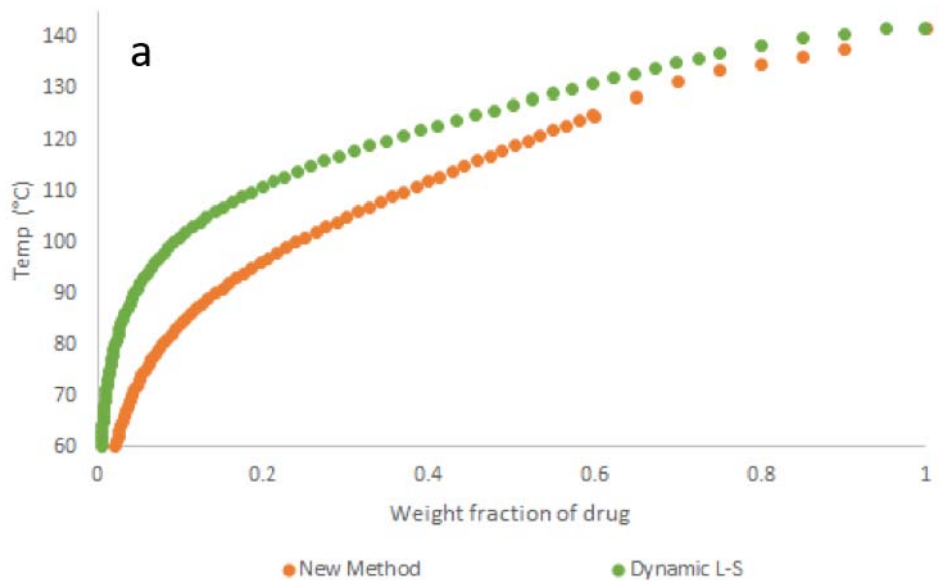


Figure 10: Plots of χ versus $1/T$ for melting point depression data determined using the dynamic method and the midpoint values of the upper and lower boundaries of the experimentally determined liquid-solid transition curve using HME, annealing and HDSC.



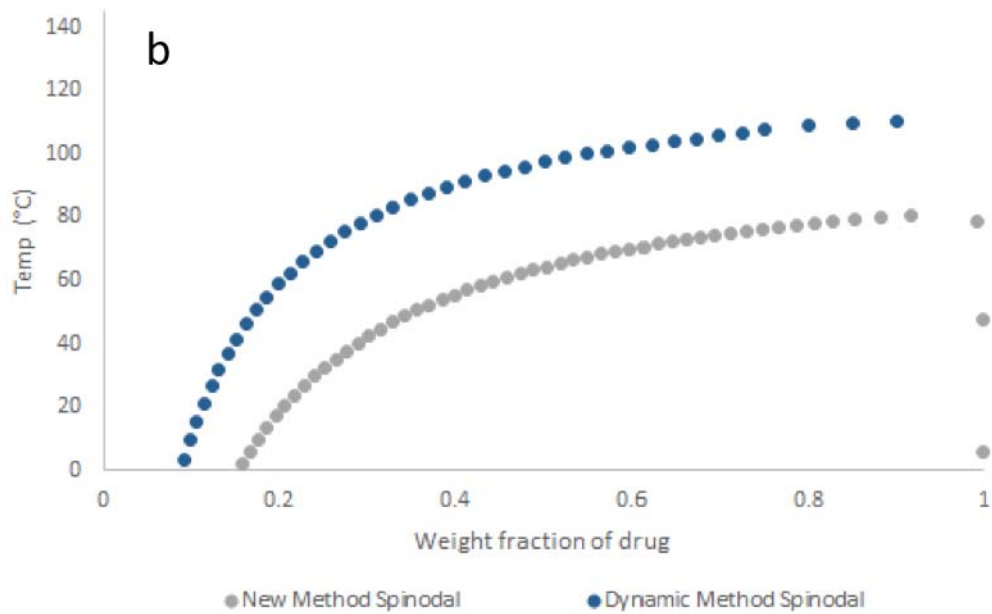


Figure 11: (a) comparison between the positions of the extrapolated liquid-solid transition curves constructed using the respective A and B values taken from figure 10; (b) calculated positions of the spinodal curves when adopting either the dynamic heating or HME, annealing and HyperDSC methodology.

References

1. Pajula, K.; Taskinen, M.; Lehto, V.; Ketolainen, J.; Korhonen, O. Predicting the Formation and Stability of Amorphous Small Molecule Binary Mixtures from Computationally Determined Flory-Huggins Interaction Parameter and Phase Diagram. *Mol. Pharm.* **2010**, *7*, 795-804.
2. Pajula, K.; Wittoek, L.; Lehto, V.; Ketolainen, J.; Korhonen, O. Phase Separation in Coamorphous Systems: in Silico Prediction and the Experimental Challenge of Detection. *Molecular Pharmaceutics* **2014**, *11*, 2271-2279.
3. Marsac, P.J.; Shamblin, S.L.; Taylor, L.S. Theoretical and practical approaches for prediction of drug-polymer miscibility and solubility. *Pharm. Res.* **2006**, *23*, 2417-2426.
4. Marsac, P.J.; Li, T.; Taylor, L.S. Estimation of Drug-Polymer Miscibility and Solubility in Amorphous Solid Dispersions Using Experimentally Determined Interaction Parameters. *Pharm. Res.* **2009**, *26*, 139-151.
5. Tian, Y.; Booth, J.; Meehan, E.; Jones, D.S.; Li, S.; Andrews, G.P. Construction of Drug-Polymer Thermodynamic Phase Diagrams Using Flory-Huggins Interaction Theory: Identifying the Relevance of Temperature and Drug Weight Fraction to Phase Separation within Solid Dispersions. *Mol. Pharm.* **2013**, *10*, 236-248.
6. Tian, Y.; Jones, D.S.; Andrews, G.P. An Investigation into the Role of Polymeric Carriers on Crystal Growth within Amorphous Solid Dispersion Systems. *Molecular pharmaceutics* **2015**,
7. Byrn, S.; Futran, M.; Thomas, H.; Jayjock, E.; Maron, N.; Meyer, R.F.; Myerson, A.S.; Thien, M.P.; Trout, B.L. Achieving Continuous Manufacturing for Final Dosage Formation: Challenges and How to Meet Them May 20-21, 2014 Continuous Manufacturing Symposium. *J. Pharm. Sci.* **2015**, *104*, 792-802.
8. Donnelly, C.; Tian, Y.; Potter, C.; Jones, D.S.; Andrews, G.P. Probing the effects of experimental conditions on the character of drug-polymer phase diagram constructed using Flory-Huggins theory. *Pharm. Res.* **2014**, *32*, 167-179.
9. Tao, J.; Sun, Y.; Zhang, G.G.Z.; Yu, L. Solubility of Small-Molecule Crystals in Polymers: d-Mannitol in PVP, Indomethacin in PVP/VA, and Nifedipine in PVP/VA. *Pharm. Res.* **2009**, *26*, 855-864.

10. Mahieu, A.; Willart, J.; Dudognon, E.; Danede, F.; Descamps, M. A New Protocol To Determine the Solubility of Drugs into Polymer Matrixes. *Molecular Pharmaceutics* **2013**, *10*, 560-566.
11. Knopp, M.M.; Olesen, N.E.; Holm, P.; Lobmann, K.; Holm, R.; Langguth, P.; Rades, T. Evaluation of drug-polymer solubility curves through formal statistical analysis: comparison of preparation techniques. *J. Pharm. Sci.* **2015**, *104*, 44-51.
12. Rumondor, A.C.F.; Ivanisevic, I.; Bates, S.; Alonzo, D.E.; Taylor, L.S. Evaluation of Drug-Polymer Miscibility in Amorphous Solid Dispersion Systems. *Pharm. Res.* **2009**, *26*, 2523-2534.
13. Rumondor, A.C.F.; Jackson, M.J.; Taylor, L.S. Effects of Moisture on the Growth Rate of Felodipine Crystals in the Presence and Absence of Polymers. *Cryst. Growth Des.* **2010**, *10*, 747-753.
14. Caron, V.; Tajber, L.; Corrigan, O.I.; Healy, A.M. A Comparison of Spray Drying and Milling in the Production of Amorphous Dispersions of Sulfathiazole/Polyvinylpyrrolidone and Sulfadimidine/Polyvinylpyrrolidone. *Mol. Pharm.* **2011**, *8*, 532-542.
15. Descamps, M.; Aumelas, A.; Desprez, S.; Willart, J.F. The amorphous state of pharmaceuticals obtained or transformed by milling: Sub-T_g features and rejuvenation. *Journal of Non-Crystalline Solids* **2015**, *407*, 72-80.
16. Qi, S.; Belton, P.; Nollenberger, K.; Gryczke, A. Compositional Analysis of Low Quantities of Phase Separation in Hot-Melt-Extruded Solid Dispersions: A Combined Atomic Force Microscopy, Photothermal Fourier-Transform Infrared Microspectroscopy, and Localised Thermal Analysis Approach. *Pharm. Res.* **2011**, *28*, 2311-2326.
17. Sun, Y.; Tao, J.; Yu, L. Solubilities of Crystalline Drugs in Polymers: An Improved Analytical Method and Comparison of Solubilities of Indomethacin and Nifedipine in PVP, PVP/VA, and PVAc. *J. Pharm. Sci.* **2010**, *99*, 4023-4031.
18. Keen, J.M.; Martin, C.; Machado, A.; Sandhu, H.; McGinity, J.W.; DiNunzio, J.C. Investigation of process temperature and screw speed on properties of a pharmaceutical solid dispersion using corotating and counter-rotating twin-screw extruders. *J. Pharm. Pharmacol.* **2014**, *66*, 204-217.
19. Li, S.; Tian, Y.; Jones, D.S.; Andrews, G.P. Optimising Drug Solubilisation in Amorphous Polymer Dispersions: Rational Selection of Hot-melt Extrusion Processing Parameters. *Aaps Pharmscitech* **2016**, *17*, 200-213.
20. Zhao, Y.; Inbar, P.; Chokshi, H.; Malick, A.W.; Choi, D. Prediction of the Thermal Phase Diagram of Amorphous Solid Dispersions by Flory-Huggins Theory. *J. Pharm. Sci.* **2011**, *100*, 3196-3207.

21. Lin, D. and Huang, Y. A thermal analysis method to predict the complete phase diagram of drug-polymer solid dispersions. *Int. J. Pharm.* **2010**, *399*, 109-115.
22. Tian, Y.; Caron, V.; Jones, D.S.; Healy, A.; Andrews, G.P. Using Flory-Huggins phase diagrams as a pre-formulation tool for the production of amorphous solid dispersions: a comparison between hot-melt extrusion and spray drying. *J. Pharm. Pharmacol.* **2013**, *66*, 256-274.
23. Coleman, M.M.; Graf, J.F.; Painter, P.C. *Specific interactions and the miscibility of polymer blends*. Technomic: Lancaster, PA, 1991;
24. Rubinstein, M. and Colby, R.H. *Polymer physics*. Oxford university press: Oxford, 2003;
25. Yang, M.; Wang, P.; Suwardie, H.; Gogos, C. Determination of acetaminophen's solubility in poly(ethylene oxide) by rheological, thermal and microscopic methods. *Int. J. Pharm.* **2011**, *403*, 83-89.
26. Qian, F.; Huang, J.; Hussain, M. Drug-Polymer Solubility and Miscibility: Stability Consideration and Practical Challenges in Amorphous Solid Dispersion Development. *J. Pharm. Sci.* **2010**, *99*, 2941-2947.
27. Hancock, B. and Zograf, G. Characteristics and significance of the amorphous state in pharmaceutical systems. *J. Pharm. Sci.* **1997**, *86*, 1-12.
28. Baird, J.A.; Van Eerdenbrugh, B.; Taylor, L.S. A Classification System to Assess the Crystallization Tendency of Organic Molecules from Undercooled Melts. *J. Pharm. Sci.* **2010**, *99*, 3787-3806.
29. Knopp, M.M.; Tajber, L.; Tian, Y.; Olesen, N.E.; Jones, D.S.; Kozyra, A.; Lobmann, K.; Paluch, K.; Brennan, C.M.; Holm, R.; Healy, A.M.; Andrews, G.P.; Rades, T. Comparative Study of Different Methods for the Prediction of Drug-Polymer Solubility. *Molecular Pharmaceutics* **2015**, *12*, 3408-3419.
30. Gramaglia, D.; Conway, B.; Kett, V.; Malcolm, R.; Batchelor, H. High speed DSC (hyper-DSC) as a tool to measure the solubility of a drug within a solid or semi-solid matrix. *Int. J. Pharm.* **2005**, *301*, 1-5.
31. Steele, G. and Austin, T. *Pharmaceutical Preformulation and Formulation*, second. *Taylor & Francis* **2009**,